Relay Selection and Power Allocation for Energy Efficiency Maximization in Hybrid Satellite-UAV Networks with CoMP-NOMA Transmission

Sedighe Mirbolouk, Morteza Valizadeh, Mehdi Chehel Amirani, Samad Ali

Abstract—Non-orthogonal multiple access (NOMA) and co-ordinated multi-point (CoMP) are two fundamental techniques considered for the fifth generation (5G) of wireless communications. In this paper, a hybrid satellite-unmanned aerial vehicle (UAV) relay network (HSURN) is proposed where the UAV relays (URs) employ CoMP transmission to serve the terrestrial users (UEs). Furthermore, all UEs associated with the CoMP-URs form a single NOMA cluster. For this model, an optimization problem is formulated subject to the minimum quality of services (QoSs) requirements of the UEs, transmission power budgets and, successive interference cancellation (SIC), to select URs and allocate their transmission powers for the energy efficiency (EE) maximization. With this insight, first, a computationally efficient sub-optimal UR selection scheme is proposed. Then, the powers are allocated to the selected URs via the Lagrange multipliers optimization (LMO) method. Due to the non-convex nature of the considered problem, it is relatively difficult to be solved. Hence, a metaheuristic teaching-learning-based optimization (TLBO) algorithm is employed to achieve an efficient solution. Simulation results are provided to verify the effectiveness of the proposed sub-optimal relay selection scheme and the TLBO-based power allocation method compared to the LMO conventional method. Besides, the obtained results also reveal that the CoMP-NOMA transmission in the proposed scenario significantly improves the spectral efficiency (SE) and outage probability (OP) of the system compared to non-comp NOMA transmission case.

Index Terms—Non-orthogonal multiple access (NOMA), Co-ordinated multi-point (CoMP) transmission, energy efficiency (EE), UAV relay selection, satellite terrestrial network, outage probability (OP).

I. INTRODUCTION

The 5G-satellite networks in the integrated architecture have emerged as a valuable infrastructure to meet the future radio access of smart devices. Combining satellite components into wireless systems is not only an indispensable way to provide seamless coverage and large capacity for users all over the world but also to ensure high QoS expectations [1]. Mobile satellite networks have been viewed as a promising technique for the smart grid, internet-of-thing (IoT), wireless sensor networks, vehicular ad-hoc networks, and massive machine-type communication. However, in situations where the line of sight (LOS) link between the satellite and ground user is blocked by obstacles, system performance significantly degrades. In this regard, UAV communications are an attractive technique that can provide better performances [2]. Despite the limited life, UAVs have recently been used as cheap relays in different conditions, especially emergencies where hybrid satellite-terrestrial relay networks are disabled. UAVs, as flying base stations (BSs) in the sky, can adjust their locations dynamically to prepare flexible and on-demand services to the terrestrial users according to their locations [3]. Therefore, to support reliable and high remote transmission rate, it is imperative to integrate UAV relays into satellite networks. UAV, NOMA, and CoMP are envisioned as critical key techniques in 5G and beyond [4], [5]. In the past generations of cellular networks, resources are orthogonal allocated to users for reducing intra-cell interference. However, the insistence on orthogonality limits the number of users who could access the network resources. NOMA merges the superposition coding technique at the transmitters with the successive interference cancellation (SIC) technique at the receivers. Thus, users can decode their signals even though they are employing the same frequency channel simultaneously. Hence, the NOMA scheme improves the spectral efficiency of users and system capacity as well as the fairness of the network [6]. In multi-cell heterogeneous network scenarios, the inter-cell interference (ICI) seriously degrades the QoS of the cell edge users. To solve this problem, NOMA should be combined with the third generation partnership project (3GPP) interference degradation techniques like CoMP to obtain higher SE. In joint transmission CoMP, the set of BSs coordinate to serve a UE simultaneously. Thus, JT-CoMP in NOMA-based downlink transmission can significantly enhance the QoS of users [7].

In this work, the application of CoMP with NOMA in HSURN is investigated. To meet the requirements of the 5G green communication and decrease the energy consumption of the URs, the relay selection and power allocation for energy efficiency are analyzed. Also, OP is employed as the criterion to show the performance of the proposed approach. We often encounter complex computations for EE maximization. Thus, efficient algorithms are necessary for the UR selection and power allocation in a way to optimize the EE in HSURN while utilizing CoMP-NOMA transmission.

Sedighe Mirbolouk, Morteza Valizadeh and Mehdi Chehel Amirani are with Electrical and Computer Engineering Department, Urmia University, Urmia, Iran (e-mail: s.mirbolouk@urmia.ac.ir, mo.valizadeh@urmia.ac.ir, m.amirani@urmia.ac.ir). Samad Ali is with Center for Wireless Communication, University of Oulu, Oulu, Finland (email: samad.ali@oulu.fi) (Correspondig author: Mehdi Chehel Amirani).

A. Prior Works

Many works on the satellite-terrestrial integrated networks (STINs) have been focused on enhancing system performance by power or resource allocation. A joint user pairing and power allocation scheme in a NOMA-based geostationary earth orbit (GEO) and low earth orbit (LEO) multi-layer satellite networks (MLSNs) was investigated in [8], in which a novel NOMA framework with two uplink receivers was considered to maximize the system capacity. In [9], the NOMA was utilized into massive multiple input multiple output (mMIMO) LEO satellite communication system (SCS) to enhance SE by considering the transmitted power, QoS constraints, imperfect SIC and imperfect channel state information (CSI). A joint beamforming design for NOMA-based cognitive STIN was presented in [10], where the satellite network and the terrestrial network employed OMA and NOMA schemes, respectively. The main idea was to maximize the sum secrecy rate of satellite UEs under the imperfect CSI, while meeting the QoS requirements of ground UEs and transmission power constraints of the cognitive STIN. In [11], maximization of the energy-efficient transmission for a STIN with a multi-antenna UR was investigated. For solving the non-convex maximization problem, two new beamforming schemes were proposed by jointly exploiting array signal processing. In [12]–[15], NOMA was employed in terrestrial networks or satellite-terrestrial links. In [12] a joint iterative algorithm was proposed to maximize the total system capacity and in [13], the exact analytical expression for the OP, and the ergodic capacity expression of the considered system were derived. In [14], the SE was improved and the decay of retrieving the content for the satellite user was reduced. The effects of both imperfect CSI and imperfect SIC were studied in [15], and its OP was evaluated. Also, the expressions of the ergodic spectral efficiency and system throughput were derived in the presence of channel estimation errors and residual interference. The performance of NOMA-based relaying-aided STIN was investigated in [16] and [17]. In [16], the SE was enhanced in the presence of multiple primary UEs under a spectrum sharing environment. In [17], the partial relay selection algorithm was employed to reach a trade-off between system performance and complexity. Also, the imperfect SIC was considered for practical constraints to derive the OP and ergodic capacity. Despite the benefits of the STINs, without considering the energy-efficient power allocation strategy in the previous papers, the STINs may not meet the increasing demands for reducing the power consumption.

The UR as an aerial BS for providing the connectivity to terrestrial UEs in the downlink NOMA system was studied in [18], and the joint trajectory design and resource allocation algorithms were investigated to maximize the minimum achievable rate of UEs. To improve the EE by power allocation optimization in a 6G enabled UR network, a combination of NOMA and spatial modulation techniques were proposed in [19]. A power allocation scheme for NOMA-UR networks with circular trajectory was proposed in [20] which maximizes the SE of common UEs subject to increase the security for a specific UE. For SE maximization, considering the limitations

on transmission power, QoS of UEs and UR's position, a joint problem of power allocation and UR's location was formulated in [21] where a harris optimization approach was proposed to solve the considered non-convex problem. A two-stage relay selection scheme for NOMA networks with decode and forward (DF) and AF protocols with different QoS requirements for the users was investigated in [22], and OP as well as diversity order were obtained. To improve the transmission reliability, a dynamic relay detection strategy was designed, which fully exploits the available side information to mitigate the inter-UE interference and maximizes the cell-center UE successful decoding probability [23]. The pre-coding optimization for UAV-assisted NOMA networks were investigated in [24] and [25]. In [24], an artificial jamming technique was utilized to guarantee security. In [25], the SE was maximized by jointly optimizing the UAV trajectory and the NOMA precoding in which the optimization problem was solved by an iterative algorithm. Actually, none of the mentioned works considered the CoMP transmission among the URs for improving the EE.

The CoMP-enabled NOMA was studied in downlink homogeneous multi-cell networks subject to increase SE [26] and to mitigate the OP [27] where cell-edge users were able to be served by CoMP-NOMA transmissions simultaneously. In [28], the integration between CoMP transmission and NOMA in the downlink heterogeneous cloud radio access networks was investigated proving that inter-cell interference and SE. The amalgamation between the reconfigurable intelligent surface technology and the JT-CoMP was analyzed to boost the ergodic rate of a cell-edge UE in a two-user NOMA cluster without decreasing the performance of the NOMA cell-center UE [29]. The combination of CoMP with mutual SIC was utilized in NOMA multi-cell networks to deteriorate the inter-cell interference and enhance the spectral efficiency of the cell-edge user [30]. A generalized coordinated multi-point transmission enabled NOMA scheme in a multi-cell network was proposed in [31], which unlike previous works improved the SINR of both cell-edge UEs and cell-centre UEs. As seen, all these reviewed researches have restricted the application of CoMP transmission in ground NOMA networks.

B. Motivation and Contributions

Despite the firm structure on air-to-ground networks and the NOMA scheme depicted in the mentioned works, there are still great research opportunities on satellite-UAV communications. To the best of our knowledge, there have been no existing works investigating CoMP among URs with downlink NOMA transmission. In this paper, a new framework for HSURN based on NOMA along with CoMP among aerial relays is proposed. Further, the EE maximization for HSURN considering joint transmission (JT) for selected URs as CoMP set is presented. Therefore, the CoMP in our work means the same as JT-CoMP. For efficient performance, the CoMP URs serve all UEs simultaneously, which significantly enhances the overall SINR performance. Also, computationally-efficient sub-optimal UR selection and power allocation algorithms are provided to maximize the EE subject to the minimum
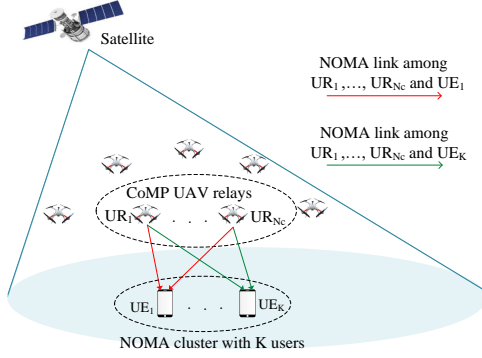
Fig. 1. CoMP-enabled NOMA in hybrid satellite-UAV relay network

SE requirements, transmission powers and, SIC constraints. The power allocation problem is solved by LMO. Since this problem is non-convex, it is mainly challenging to tackle it. Therefore, the TLBO algorithm is utilized to achieve an efficient solution. Further, an analytical expression for the OP of the network is presented. Finally, the network performance for URs in various heights is evaluated, and the EE of the suggested sub-optimal solution is compared to the optimal one.

The main contributions of our work are listed as follow:

- Introducing a new framework for HSURN based on the downlink NOMA transmission and CoMP among URs
- Problem formulation for UR selection and power allocation to maximize the EE in the suggested transmission scheme
- Employing a convex relaxed method based on a meta-heuristic algorithm for optimization problem besides the Lagrange multipliers optimization method
- Deriving analytical results for the OP of the system

C. Organization and Notation

The rest of this paper is organized as follows: Section II describes the system model of the proposed framework in downlink transmission. Section III characterizes the relay selection scheme and the power allocation algorithms. Section IV discusses the computational complexity. Section V provides the outage performance of the proposed model. section VI verifies the numerical results and finally, section VII concludes the paper.

Notation: Scalars are depicted by small letters, vectors and matrices are shown by bold and capital letters, respectively. For a value x, $|x|$ denotes its absolute value.

II. COMP-ENABLED NOMA HSURN MODEL

The proposed HSURN based on downlink NOMA transmission along with CoMP among URs is illustrated in Fig. 1. A satellite (S) simultaneously communicates with K single antenna terrestrial UEs that are randomly distributed. The communication is aided by J single antenna URs. The indices for the UEs and URs are defined as $k \in \{1, 2, ..., K\}$ and $j \in \{1, 2, ..., J\}$. It is assumed that URs and UEs are located in the same spot beam of the satellite. In practical scenario, because of the existence of obstacles, the links between satellite

and terrestrial UEs are usually non-line of sight (NLOS). Thus, UEs cannot be well covered by the satellite individually, and their accessible SINRs are usually very low. Hence, UAVs as aerial relays above UEs is employed to decode and forward the wireless signals transmitted by satellite. All URs are connected and have the ability of CoMP. Since the S-URs and URs-UEs links are somewhat LOS, and also URs are CoMP-enabled, the SINR of the UEs is significantly improved. Every UE can be served by N_c URs which refers to the CoMP order. As well as, NOMA is incorporated into JT-CoMP-URs to further improve the SINR of UEs. All the UEs associated with the CoMP URs form a NOMA set. As illustrated in Fig. 1, the satellite transmits signals to the URs in the first time slot. Then, the selected URs decode and retransmit the signals to all UEs. In the power domain NOMA, there is a difference in the power levels of the received signals from URs. Hence, UEs decode the signals by applying the SIC technique. Two UE categories are considered: the weak UEs and the strong UEs. The weak users have poor channel conditions, while the strong users have better channel conditions. Fig.1 shows CoMP transmission based on the relay selection scheme which is described in section III. Perfect CSI is considered to be available at all nodes.

Let $h_{s,j}$ represents the channel power gain from the satellite to UR_j and follows shadowed-Rician fading distribution, i.e. $h_{s,j} = h'_{s,j} + h''_{s,j}$. The LOS component $h'_{s,j}$ follows Nakagami-m' distribution, $h'_{s,j} \sim$ Nakagami (m', Ω') with the fading parameter m' and the average power of the LoS component Ω'. The entries of the scattering components $h''_{s,j}$ follow Rayleigh distribution, $h''_{s,j} \sim$ Rayleigh (b''), where $2b''$ is the average power of the scatter component [32]. Let $h_{j,k}$ represents the channel power gain from the UR_j to the UE_k which, $h_{j,k} = L_{j,k}\hat{h}_{j,k}$. The free space loss is set to $L_{j,k} = d_{j,k}^{-\alpha/2}$, where, α denotes the path loss exponent and $d_{j,k} = \sqrt{d_{h,j}^2 + d'^2_{j,k}}$, where, $d_{h,j}$ is the height of UR_j and $d'_{j,k}$ is the distances between the vertical projections of UR_j and UE_k. In channel fading model the $UR_j - UE_k$ link, $\hat{h}_{j,k}$ is independent and identically distributed (i.i.d) Nakagami-$\hat{m}$ distribution, $\hat{h}_{j,k} \sim$ Nakagami $(\hat{m}, \hat{\Omega})$ [33].

Satellite broadcasts signal x_s with transmission power p_s, the received signal at each UR is $y_j = \sqrt{p_s}h_{s,j}x_s + n_j$, where x_s includes desired signals of users and n_j is the additive white Gaussian noise (AWGN) of the UR_j link with the standard deviation of the $\sigma_{j,k}$. It is assumed that the selected URs for CoMP set, i.e., $j_c \in \{1, 2, ..., N_c\}$, adopt the NOMA principle. The URs transmit the signals to UEs based on the NOMA strategy. Hence, superposition coding at the URs and SIC at the users are utilized in this way the users can be multiplexed on the same sub-band. In other words, the URs employ a specific sub-band for all UEs. The UEs with higher SIC ordering can decode and remove the interference signal of the users who have lower SIC ordering. Thus, UE_k receives the following signal:

$$z_k = \sum_{j_c \in S_c} (\sqrt{p_{j_c,k}}\, x_{j_c,k} + \sum_{t=k+1}^{K} \sqrt{p_{j_c,t}}\, x_{j_c,t})\tilde{h}_{j_c,k} + n_k, \quad (1)$$

where S_c shows the CoMP set, $p_{j_c,k}$ and $x_{j_c,k}$ are the allocated power and the modulated symbol to UE_k by UR_{j_c}, respectively, $\tilde{h}_{j_c,k} = \dfrac{|h_{j_c,k}|^2}{\sigma_{j_c,k}^2}$ is the normalized square channel gain, $\tilde{h}_{j_c,k} \sim \text{Gamma}\,(a_{j_c,k}, b_{j_c,k})$ where $a_{j_c,k} = \hat{m}$, $b_{j_c,k} = \dfrac{\sigma_{j_c,k}^2 \hat{m}}{|L_{j_c,k}|^2 \hat{\Omega}}$ and n_k is AWGN. The first term in (1) represents the received signal transmitted from the UR_{j_c} at the UE_k. The second term is the interference caused by the transmitted signal to UEs with higher SIC order compared to the UE_k. In general, the SIC order of the UEs is different for the URs, only those URs can be selected for CoMP transmission that the SIC order of each UE is the same for all of them [26]. Therefore, the normalized channel gains between the UE_k and the selected UR_{j_c} are sorted as $|\tilde{h}_{j_c,1}| \leq |\tilde{h}_{j_c,2}| \leq ... \leq |\tilde{h}_{j_c,K}|$. Hence, the total sum-rate/spectral efficiency of the UEs can be expressed as

$$R_{sum} = \sum_{k=1}^{K} R_k = \sum_{k=1}^{K} \log_2(1 + \gamma_k), \qquad (2)$$

where R_k is the achievable rate for the UE_k after SIC operation and γ_k is the SINR at the UE_k as follow:

$$\gamma_k = \frac{\displaystyle\sum_{j_c=1}^{N_c} p_{j_c,k}\tilde{h}_{j_c,k}}{\displaystyle\sum_{j_c=1}^{N_c} \sum_{t=k+1}^{K} p_{j_c,t}\tilde{h}_{j_c,k} + 1}, \qquad (3)$$

To reach R_k at the UE_k, the UEs with a higher order of SIC should be able to decode the message of UE_k. In other words, for successful SIC operation at the UE_k, it is necessary for all UE_f to satisfy [34]:

$$R_k^f = \log_2\left(1 + \frac{\displaystyle\sum_{j_c=1}^{N_c} p_{j_c,k}\tilde{h}_{j_c,f}}{\displaystyle\sum_{j_c=1}^{N_c} \sum_{t=k+1}^{K} p_{j_c,t}\tilde{h}_{j_c,f} + 1}\right) \geq R_k^{th}$$
$$\forall f = k+1, 2, ..., K, \qquad (4)$$

where R_k^f is the rate of the UE_f to decode the message of the UE_k, and R_k^{th} is a threshold data rate for UE_k. On the other hand, (4) can be reduced to:

$$\sum_{j_c=1}^{N_c} p_{j_c,k}\tilde{h}_{j_c,k+1} - \sum_{j_c=1}^{N_c} \sum_{t=k+1}^{K} p_{j_c,t}\tilde{h}_{j_c,k+1} - 1 \geq \delta$$
$$\forall k = 1, 2, ..., K-1, \qquad (5)$$

where δ is the least difference between the power of decoded signal and inter-NOMA-user interference [26], [35]. The Eq. (5) will be considered as SIC constraints in our optimization problem.

III. PROPOSED RELAY SELECTION AND POWER ALLOCATION

In this section, the relay selection and power allocation problem is formulated mathematically to maximize the entire system EE under NOMA power budget, QoS requirement, and SIC constraint. EE is defined by dividing the SE by the total power consumption:

$$\eta_{EE} = \frac{R_{sum}}{\displaystyle\sum_{j_c=1}^{N_c} \sum_{k=1}^{K} p_{j_c,k} + p_{cir}}, \qquad (6)$$

where p_{cir} is the circuit power of the system.

In the following, firstly, the relay selection scheme is presented and then, the power allocation is discussed.

A. Relay Selection Scheme

For the HSURN, the aim of the optimal relay selection algorithm is the assurance of successful transmission of the UEs signals as well as maximization of the EE that provides reliable transmission for the system. The algorithm runs through three stages.

stage 1: A subset of existing URs, S_r, is selected that can guarantee successful reception in the S-URs links and prepare reliable signal forwarding to UEs. All the URs in S_r need to satisfy the decoding threshold rate of the UEs desired signals, i.e., $S_r = \{UR_j | R_j \geq R_{min}\}$, where R_j presents the achievable rate at UR_j. If S_r is empty, none of the URs can provide successful signal transmission to the UEs. Therefore, there is no candidate UR for the next selection stage. In contrast, if S_r is not empty and at least N_c URs can satisfy the transmission conditions, the next stage of the UR selection will be performed.

stage 2: This stage tries to solve the challenge of the NOMA principle to determine the appropriate SIC ordering of UEs. In the CoMP transmission, several URs using the specific resource block at the same time send multiple streams of equal data to each UE. The UEs and the CoMP-URs set form a NOMA cluster that makes them experience inter-NOMA-user interference (INUI) depending on their SIC ordering. As mentioned before, for each UE, having the same SIC ordering with respect to all URs is necessary. Hence, from the S_r, those URs which satisfy this constraint are selected and placed in the new set, S_o. Each UE may experience different channel conditions, i.e., weak or strong channel gains, thus, different SIC orders can be considered for it. In this work, we consider a SIC ordering based on the required QoS of the UEs, in which, the URs in S_o are selected so that a user with a higher QoS has a higher SIC order (stronger channel gains) compared to others.

stage 3: For achieving the optimal selection, it is necessary to investigate the EE of UEs for all possible N_c-combination of S_o, $\binom{|S_o|}{N_c}$, where $|S_o|$ is the cardinality of the set of all existing URs, S_o. The subset of URs which leads to the maximum value of EE is considered as S_c. Due to the delay and high complexity caused in the optimal selection, a sub-optimal relay selection is proposed, which its results are close to the results of the optimal case with less complexity. In this situation, the N_c UAV relays with highest sum of their channel fading gain, $\sum_{k=1}^{K} \tilde{h}_{j,k}$, is selected as S_c among S_o. The stages of UR selection are summarized in Algorithm 1.

Algorithm 1 Pseudo-code of the proposed sub-optimal relay selection scheme

1: **Initialize** $S_r = S_o = S_c = \phi$
2: **for** $j = 1$ to J **do**
3:   **if** $(R_j \geq R_{min})$ **then**
4:     $S_r = S_r \cup UR_j$
5:     **if** $(\tilde{h}_{j,k} < \tilde{h}_{j,k+1}, \ \forall k \in 1, 2, ..., K-1)$ **then**
6:       $S_o = S_o \cup UR_j$
7:     **end if**
8:   **end if**
9: **end for**
10: Select N_c relays with highest $\sum_{k=1}^{K} \tilde{h}_{j,k}$ as S_c

B. Power Allocation Scheme

To maximize the EE of CoMP-URs, the power allocation problem can be formulated as:

$$\{p^*_{j_c,k}\} = \underset{\{p_{j_c,k}\}}{\arg \max}(\eta_{EE}) \qquad (7)$$

subject to:

$$C_1 : \sum_{k=1}^{K} p_{j_c,k} \leq p_{tot}, \ \forall j_c = 1, 2, ..., N_c$$

$$C_2 : p_{j_c,k} \geq p_{min}, \ \forall j_c = 1, 2, ..., N_c, \ k = 1, 2, ..., K$$

$$C_3 : R_k \geq R_{k,min}, \ \forall k = 1, 2, ..., K$$

$$C_4 : \sum_{j_c=1}^{N_c} p_{j_c,k} \tilde{h}_{j_c,k+1} - \sum_{j_c=1}^{N_c} \sum_{t=k+1}^{K} p_{j_c,t} \tilde{h}_{j_c,k+1} - 1 \geq \delta$$

$$\forall k = 1, 2, ..., K-1,$$

where $\left\{p^*_{j_c,k}\right\}$ shows the optimum transmission powers set of the CoMP-URs to the UEs. C_1 and C_2 show the transmission power budget constraints. C_3 gives the basic rate requirement of each NOMA UE and C_4 represents the SIC constraint.

The EE maximization problem formulated in (7) is a power allocation problem among the CoMP-URs. Therefore, for each desired and specified UR from the CoMP set, for example, $UR_{\hat{j}_c}$, it is required the problem (7) to be solved in view of all the feasible solutions for other URs of set S_c. Thus, the power allocation of $UR_{\hat{j}_c}$ is optimized as follows:

$$\{p^*_{\hat{j}_c,k}\} = \underset{\{p_{\hat{j}_c,k}\}}{\arg \max}(\eta_{EE}) \qquad (8)$$

subject to:

$$C_1 : \sum_{k=1}^{K} p_{\hat{j}_c,k} \leq p_{tot}$$

$$C_2 : p_{\hat{j}_c,k} \geq p_{min}, \ k = 1, 2, ..., K$$

$$C_3 : R_k \geq R_{k,min}, \ \forall k = 1, 2, ..., K$$

$$C_4 : \sum_{j_c=1}^{N_c} p_{j_c,k} \tilde{h}_{j_c,k+1} - \sum_{j_c=1}^{N_c} \sum_{t=k+1}^{K} p_{j_c,t} \tilde{h}_{j_c,k+1} - 1 \geq \delta$$

$$\forall k = 1, 2, ..., K-1,$$

The above problem is solved by two different methods; LMO and TLBO. Because of the non-convex nature of this problem the standard LMO method is relatively challenging. Hence, a convex relaxation meta-heuristic algorithm, TLBO, is examined to find an efficient solution. Unlike the conventional solutions like gradient-based methods, TLBO does not utilize the gradient of the objective functions. Also, its implementation is straightforward, and it is capable of escaping local optima.

C. Lagrange Multiplier Optimization Method

The formulated optimization problem (8) is a nonlinear fractional programming. It can be transformed into an equivalent concave non-fractional form as follows [36]:

$$q^* = \underset{\{p_{\hat{j}_c,k}\}}{\max}\left(\frac{R_{sum}}{\sum_{j_c=1}^{N_c}\sum_{k=1}^{K} p_{\hat{j}_c,k} + p_{cir}}\right) = $$
$$\frac{R_{sum}(\{p^*_{\hat{j}_c,k}\})}{\sum_{k=1}^{K} p^*_{\hat{j}_c,k} + \sum_{\substack{j_c=1 \\ j_c \neq \hat{j}_c}}^{N_c}\sum_{k=1}^{K} p_{j_c,k} + p_{cir}}. \qquad (9)$$

Considering (9), subtractive transformation of the problem in (8) subject to $C_1 - C_4$ can be shown as:

$$p^*_{\hat{j}_c,k} = \underset{p_{\hat{j}_c,k}}{\arg \max}(R_{sum} - q(\sum_{j_c=1}^{N_c}\sum_{k=1}^{K} p_{j_c,k} + p_{cir})). \qquad (10)$$

where q is a scaling parameter for the weight of the total power consumption of URs. For traceability of the problem, the lower bound is utilized to obtain the optimal solution iteratively. Considering the lower bound achieved in [37], the data rate of UEs can be expressed as:

$$R'_k = c_k \log_2(\gamma_k) + d_k \leq R_k = \log_2(1 + \gamma_k), \qquad (11)$$

where $c_k = \frac{\hat{\gamma}_k}{1+\hat{\gamma}_k}$, $d_k = \log_2(1 + \hat{\gamma}_k) - c_k \log_2(\hat{\gamma}_k)$ and $\hat{\gamma}_k$ is the SINR of UE_k from the last iteration. Thus, problem (10) can be transformed to:

$$p^*_{\hat{j}_c,k} = \underset{\{p_{\hat{j}_c,k}\}}{\arg \max}(\sum_{k=1}^{K} R'_k - q(\sum_{j_c=1}^{N_c}\sum_{k=1}^{K} p_{j_c,k} + p_{cir})) \qquad (12)$$

subject to:

$$C_1, C_2, C_4$$
$$C_3 : R'_k \geq R_{k,min}, \ \forall k = 1, 2, ..., K,$$

Dinkelbach iterative algorithm [38] is utilized to solve (12) assuming initial value for q is small. The concavity of the above problem is proved in Appendix. Hence, according to the Karush-Kuhn-Tucker (KKT) conditions [39] the Lagrangian function of the problem (12) can be written as:

$$L(\{p_{\hat{j}_c,k}\}, q, \alpha, \boldsymbol{\beta}, \boldsymbol{\lambda}, \boldsymbol{\zeta})$$

$$= \sum_{k=1}^{K} R'_k - q\left(\sum_{j_c=1}^{N_c} \sum_{k=1}^{K} p_{j_c,k} + p_{cir}\right)$$

$$+ \alpha\left(p_{tot} - \sum_{k=1}^{K} p_{\hat{j}_c,k}\right)$$

$$+ \sum_{k=1}^{K} \beta_k(p_{\hat{j}_c,k} - p_{min})$$

$$+ \sum_{k=1}^{K} \lambda_k(R'_k - R_{k,min})$$

$$+ \sum_{k=1}^{K-1} \zeta_k\left(\sum_{j_c=1}^{N_c} p_{j_c,k}\tilde{h}_{j_c,k+1}\right.$$

$$\left. - \sum_{j_c=1}^{N_c} \sum_{t=k+1}^{K} p_{j_c,t}\tilde{h}_{j_c,k+1} - 1 - \delta\right), \quad (13)$$

where $\alpha \geq 0$, $\boldsymbol{\beta} \geq 0$, $\boldsymbol{\lambda} \geq 0$ and $\boldsymbol{\zeta} \geq 0$ are the Lagrange multipliers of constraints on the transmission power, SE and SIC limitation, respectively. The problem in (14) can be decomposed into a maximization and a minimization sub-problem. The maximization sub-problem finds the optimal power allocation and then the results is minimized to obtain the optimal Lagrange multipliers as follow:

$$\min_{q,\alpha,\boldsymbol{\beta},\boldsymbol{\lambda},\boldsymbol{\zeta}} \max_{\{p_{\hat{j}_c,k}\}} L(\{p_{\hat{j}_c,k}\}, q, \alpha, \boldsymbol{\beta}, \boldsymbol{\lambda}, \boldsymbol{\zeta}). \quad (14)$$

By taking the partial derivative of the above problem with respect to $p_{\hat{j}_c,k}$, we have

$$\frac{\partial L(p_{\hat{j}_c,k}, q, \alpha, \boldsymbol{\beta}, \boldsymbol{\lambda}, \boldsymbol{\zeta})}{\partial p_{\hat{j}_c,k}}$$

$$= \frac{-1}{ln2} \sum_{\nu=1}^{k-1} c_\nu(1+\lambda_\nu) \frac{\tilde{h}_{\hat{j}_c,\nu}}{\sum\limits_{j_c=1}^{N_c} \sum\limits_{t=\nu+1}^{K} p_{j_c,t}\tilde{h}_{j_c,\nu} + 1}$$

$$+ \frac{1}{Ln2} c_k(1+\lambda_k) \frac{\tilde{h}_{\hat{j}_c,k}}{p_{\hat{j}_c,k}\tilde{h}_{\hat{j}_c,k} + \sum\limits_{\substack{j_c=1 \\ j_c \neq \hat{j}_c}}^{N_c} p_{j_c,k}\tilde{h}_{j_c,k}}$$

$$+ (q + \alpha - \beta_k) + \zeta_k\tilde{h}_{\hat{j}_c,k+1} - \sum_{\nu=1}^{k-1} \zeta_\nu\tilde{h}_{\hat{j}_c,\nu+1}. \quad (15)$$

where $(\zeta_k\tilde{h}_{\hat{j}_c,k+1} = 0$ for $k = K)$. By setting (15) to zero, the power allocation along with a fixed point policy of $UE_k(k \neq K)$ can be achieved as (16).

The outer layer in problem (14) can be solved by the gradient method. Hence, the Lagrange multipliers are calculated as follows:

$$\alpha(l+1) = \left[\alpha(l) - s(l) \times \left(p_{tot} - \sum_{k=1}^{K} p_{\hat{j}_c,k}\right)\right]^+$$

$$\beta_k(l+1) = \left[\beta_k(l) - s(l) \times (p_{\hat{j}_c,k} - p_{min})\right]^+$$

$$\lambda_k(l+1) = \left[\lambda_k(l) - s(l) \times (R'_k - R_{k,min})\right]^+$$

$$\zeta_k(l+1) = \zeta_k(l) - s(l) \times \left(\sum_{j_c=1}^{N_c} p_{j_c,k}\tilde{h}_{j_c,k+1}\right.$$

$$\left. - \sum_{j_c=1}^{N_c} \sum_{t=k+1}^{K} p_{j_c,t}\tilde{h}_{j_c,k+1} - 1 - \delta\right), \quad \forall k = 1, 2, ..., K-1, \quad (17)$$

where $[x]^+ \overset{\Delta}{=} \max\{0, x\}$. The positive value step size at iteration l, $s(l)$, is obtained based on a trade-off between the optimally and convergence speed. The algorithm keeps improving the Lagrange multipliers at each iteration until it converges to the optimum EE, i.e., the condition $\left(\sum\limits_{k=1}^{K} R'_k - q(\sum\limits_{j_c=1}^{N_c} \sum\limits_{k=1}^{K} p_{j_c,k} + p_{cir})\right) \leq \varepsilon$ is satisfied, where ε is the maximum tolerance.

D. Teaching-Learning-Based Optimization

The TLBO is a population-based meta-heuristic algorithm inspired by the cooperation among teacher and students/learners. Generally, it can be utilized for any continuous unconstrained and constrained optimization problem. Mathematically, solving the problem by TLBO can be modeled in two main stages: 1) teaching stage, and 2) learning stage [40]. Due to several constraints, adjusting the problem (8) is necessary. Hence, a constraint-handling approach in the following is utilized for transforming the problem (8) into a suitable form. The TLBO model uses N_{pop} learners that denoted as $\mathbf{p}_n = [p_{n,1}, p_{n,2}, ..., p_{n,K}]$, $n \in \{1 : N_{pop}\}$. The vector $\mathbf{p}_n$ consists of K design variables, and each variable, $p_{n,k}$, corresponds to an allocated power value. In the initialization stage the value of $p_{n,k}$ is randomly assigned satisfying the SIC constraint, i.e., $p_{n,k} \geq p_{n,k+1}$. The corresponding fitness function, f_n, related to the objective function in (8) is calculated via (23). Both of teaching and learning stages is executed at each iteration that described in the following.

1) Teaching stage

In this stage, a teacher, $\mathbf{p}^T$, tries to updates the mean value of the class in the corresponding taught subject. Since the teacher is usually a highly learned person who trains other learners for improving the class results, the algorithm considers the best-identified learner n^* as the teacher:

$$\mathbf{p}^T = \mathbf{p}_{n^*}^i, \quad \{n^* = \arg\max_n(f_n^i)\}, \quad (18)$$

and its corresponding fitness value as the best fitness function in the iteration i, f_{best}^i. The average value of the learners is determined as follows:

$$\bar{\mathbf{p}}^i = \frac{1}{N_{pop}} \sum_{n=1}^{N_{pop}} (\mathbf{p}_n^i), \quad (19)$$

$$p_{\hat{j}_c,k}^* = \frac{c_k(1+\lambda_k)}{ln2(q + \alpha - \beta_k - \zeta_k\tilde{h}_{\hat{j}_c,k+1}) + \sum_{\nu=1}^{k-1}(\zeta_k\tilde{h}_{\hat{j}_c,\nu+1} + \frac{c_\nu(1+\lambda_\nu)\tilde{h}_{\hat{j}_c,\nu}}{\sum_{j_c=1}^{N_c}\sum_{t=\nu+1}^{K}p_{j_c,t}\tilde{h}_{j_c,\nu}+1})} - \frac{\overset{\underset{j_c \neq \hat{j}_c}{j_c=1}}{\sum^{N_c}}p_{j_c,k}\tilde{h}_{j_c,k}}{\tilde{h}_{\hat{j}_c,k}}. \tag{16}$$

where $\mathbf{p}_n^i$ is the allocated power vector of learner n in iteration i. Then, it is weighted by the teaching factor t_n by taking values either 1 or 2 [41]. Because the t_n is selected randomly, it is not considered as the algorithm parameter. The knowledge difference between the class weighted average, $t_n\bar{\mathbf{p}}^i$, and teacher is weighted by a random value r_n from [0,1]. Considering this difference, the learner knowledge is updated in teaching action as follows:

$$\mathbf{p}_{n,new} = p_{n,k}^i + r_n(\mathbf{p}^T - t_n\bar{\mathbf{p}}^i). \tag{20}$$

The output of the teaching stage, $\mathbf{p}_{n,out}^T$ and $f_{n,out}^T$ is equal to the updated values if the fitness function is improved (lines 14,15 of Algorithm 2). Among the solutions of all populations, the one who obtains the best fitness function value is named as the best solution (lines 16,17). The outputs of this stage are considered as the inputs for the next learning stage.

2) Learning stage

In this stage, learners increase their knowledge by interacting with themselves. A learner interacts randomly with other learners to enhance his knowledge. A learner learns new things if an other learner is better than he. Suppose learner n wants to interact with learner m which is randomly selected $m \neq n$. For this end, the difference of knowledge between two learners is determined as follows:

$$\triangle\mathbf{p} = \begin{cases} \mathbf{p}_{m,out}^T - \mathbf{p}_{n,out}^T & f_{m,out}^T > f_{n,out}^T \\ \mathbf{p}_{n,out}^T - \mathbf{p}_{m,out}^T & otherwise, \end{cases} \tag{21}$$

The next step is to calculate a new value for each learner, $\mathbf{p}_{new}$, based on $\Delta\mathbf{p}$ as follows:

$$\mathbf{p}_{n,new} = \max\{p_{\min}, \mathbf{p}_{n,out}^T + r_n\Delta\mathbf{p}\}. \tag{22}$$

The updating process performs similarly to the teaching stage.

The teaching and learning stages are iteratively continued until TLBO algorithm convergences to the optimal power and energy. The steps of TLBO optimization are summarized in Algorithm 2.

3) Constraint-handling approach

Several constraints exist in our problem formulated in (8). Hence, a penalty mechanism is presented to deal with the constraints. The aim of the penalty mechanism is to create a fitness function such that the constrained problem (8) is transformed into an unconstrained problem. Thus, the penalty function is defined as:

$$f_n^i = \eta_{EE}(\mathbf{p}_n^i) - G(\mathbf{p}_n^i), \tag{23}$$

where $G(\mathbf{p}_n^i)$ is the penalty function and can be calculated as:

$$G(\mathbf{p}_n^i) = \sum_{z=1}^{4} w_z g_z \tag{24}$$

in which:

$$g_1 = ([p^{tot} - \sum_{k=1}^{K} p_{n,k}]^-)^2$$

$$g_2 = \sum_{k=1}^{K} ([p_{n,k} - p_{min}]^-)^2$$

$$g_3 = \sum_{k=1}^{K} ([R_{n,k} - R_{k,min}]^-)^2$$

$$g_4 = \sum_{k=1}^{K-1} ([\sum_{j_c=1}^{N_c} p_{j_c,k}\tilde{h}_{j_c,k+1} -$$

$$\sum_{j_c=1}^{N_c} \sum_{t=k+1}^{K} p_{j_c,t}\tilde{h}_{j_c,k+1} - 1 - \sigma]^-)^2$$

where w_z is penalty factor and $[x]^- \overset{\Delta}{=} \min\{0, x\}$.

IV. COMPUTATIONAL COMPLEXITY

In this section, the computational complexity of power allocation steps through LMO and TLBO algorithms is investigated for each UR. In both algorithms, each UR requires to solve the problem for all feasible answers of others.

As described before, the dual problem in (14) is decomposed into two parts. It is supposed that the counts of iterations for inner part, i.e., the power allocation maximization and outer part, i.e., Lagrange multiplier minimization is denoted by I_{max} and L_{max}, respectively. For Lagrange calculations, $I_{max}L_{max}(K(N_c - 1) + \sum_{k=1}^{K}(4k + (N_c - 1) + \sum_{v=1}^{k-1}(K - v - 1)) - 1)$ additions, $I_{max}L_{max}(K(N_c - 1) + N_c\sum_{k=1}^{K}(3k + (N_c\sum_{v=1}^{k-1}(K - v))))$ multiplications and $I_{max}L_{max}K$ comparisons are needed for inner part. In the outer part, totally $I_{max}L_{max}(8K + N_c(K - 1) + (N_c - 1)\sum_{k=1}^{K-1}(K - k - 1) - 7)$ additions, $I_{max}L_{max}(3K + N_c(K-1) + N_c\sum_{k=1}^{K-1}(K-k))$ multiplications, and $I_{max}L_{max}K$ are required. The TLBO-based method, that is represented in Algorithm 2, needs $I_{max}(3N_{pop} - 1)K$ additions, $2I_{max}N_{pop}K$ multiplications and $I_{max}N_{pop}(K+3)$ comparisons in teaching stage; and $2I_{max}N_{pop}K$ additions, $I_{max}N_{pop}K$ multiplications and $I_{max}N_{pop}(K + 3)$ comparisons in learning stage. Therefore, the total complexity order of LMO and TLBO algorithms is $O(M^{N_c-1}I_{max}L_{max}N_cK^2)$ and $O(M^{N_c-1}I_{max}N_{pop}K)$, respectively. The results were summarized in the table I and table II.

TABLE I
COMPUTATIONAL COMPLEXITY OF THE LMO METHOD

	Inner Maximization	Outer Minimization
Number of additions	$I_{max}L_{max}\left(K(N_c-1)+\sum_{k=1}^{K}[4k+(N_c-1)\right.$ $\left.\times\sum_{v=1}^{k-1}(K-v-1)]-1\right)$	$I_{max}L_{max}\left(8K+N_c(K-1)\right.$ $\left.+(N_c-1)\sum_{k=1}^{K-1}(K-k-1)-7\right)$
Number of multiplications	$I_{max}L_{max}\left(K(N_c-1)+\sum_{k=1}^{K}[3k\right.$ $\left.+N_c\sum_{v=1}^{k-1}(K-v)]\right)$	$I_{max}L_{max}\left(3K+N_c(K-1)\right.$ $\left.+N_c\sum_{k=1}^{K-1}(K-k)\right)$
Number of comparisons	$I_{max}L_{max}K$	$I_{max}L_{max}K$
Order of total complexity (Inner and Outer)	$O(M^{\bar{N}_c-1}I_{max}L_{max}N_cK^2)$	

TABLE II
COMPUTATIONAL COMPLEXITY OF THE TLBO METHOD

	Teaching stage	Learning stage
Number of additions	$I_{max}(3N_{pop}-1)K$	$2I_{max}N_{pop}K$
Number of multiplications	$2I_{max}N_{pop}K$	$I_{max}N_{pop}K$
Number of comparisons	$I_{max}N_{pop}(K+3)$	$I_{max}N_{pop}(K+3)$
Order of total complexity (Teaching and Learning)	$O(M^{\bar{N}_c-1}I_{max}N_{pop}K)$	

V. OUTAGE PROBABILITY

In this section, a closed-form expression for the OP of the proposed system is derived. The OP is defined as the probability of the instantaneous achievable SINR in the NOMA users falling below a threshold. Low values of OP show the reliable link between URs and UEs. Thus, information about the state of the communication system can be provided.

The UE_k will be in the outage if it fails to decode its signal successfully or the SIC process cannot be performed correctly. So, the successful detection probability of UE_k can be formulated as [31]:

$$P_{suc,k}=P_r\left(\gamma_{\mu\to k}>\gamma_{th}\right);\quad 1\le\mu\le k, \quad (25)$$

where $\gamma_{th}=2^{R_{\min}}-1$ is the decoding threshold, considered the same for simplicity. According to the principle of NOMA, user k decodes z_k from received signal by treating z_μ as interference. The decoding SINR $\gamma_{\mu\to k}$ can be written as

$$\gamma_{\mu\to k}=\frac{\sum_{j_c=1}^{N_c}p_{j_c,\mu}\tilde{h}_{j_c,k}}{\sum_{j_c=1}^{N_c}\sum_{t=\mu+1}^{K}p_{j_c,t}\tilde{h}_{j_c,k}+1}. \quad (26)$$

If $\gamma_{\mu\to k}>\gamma_{th}$ holds for the smallest SINR, i.e., $\min_\mu\{\gamma_{\mu\to k}\}>\gamma_{th}$, then, it will hold for the rest, thus, $P_{suc,k}$ become

$$P_{suc,k}=P_r\left(\min_\mu\{\gamma_{\mu\to k}\}>\gamma_{th}\right)$$
$$=P_r\left(\min_\mu\left(\sum_{j_c=1}^{N_c}\tilde{h}_{j_c,k}(p_{j_c,\mu}\right.\right. \quad (27)$$
$$\left.\left.-\sum_{t=\mu+1}^{K}p_{j_c,t}\gamma_{th})-\gamma_{th}\right)>0\right).$$

By considering the same power allocation for all transmitters, $p_{j_c,\mu}=p_\mu$ and $\sum_{t=\mu+1}^{K}p_{j_c,t}=\sum_{t=\mu+1}^{K}p_t$, we have:

$$P_{suc,k}=P_r\left(\sum_{j_c=1}^{N_c}\tilde{h}_{j_c,k}\min_\mu\left(p_\mu-\sum_{t=\mu+1}^{K}p_t\right)>\gamma_{th}\right). \quad (28)$$

After some straightforward calculations, the following equation is obtained:

$$P_{suc,k}=1-P_r\left(\sum_{j_c=1}^{N_c}\tilde{h}_{j_c,k}\le\frac{\gamma_{th}}{\max_\mu\left(p_{j_c,\mu}-\sum_{t=\mu+1}^{K}p_{j_c,t}\gamma_{th}\right)}\right), \quad (29)$$

thus, the probability of successful signal detection at UE_k can be expressed as:

$$P_{suc,k}=1-F_{h_k}(h_0), \quad (30)$$

Algorithm 2 Pseudo-code of the TLBO algorithm

1: **Initialize** I_{max}, ε *and* N_{pop}
2: set i=1
3: **for** $n = 1$ to N_{pop} **do**
4:    Initialize $\mathbf{p}_n^i$ such that $p_{n,k}^i \geq p_{n,k+1}^i$; $k = \{1, 2, ..., K - 1\}$
5:    Calculate f_n^i according to (23)
6: **end for**
7: Initialize $\mathbf{p}_{best}^i = \mathbf{p}_{n*}^i$ according to (18) and $f_{best}^i = f_{n*}^i$
8: **while** $i \leq I_{\max}$ **do**
9:    $\triangleright$ Teaching stage
10:    Calculate $\bar{\mathbf{p}}^i$
11:    set $\mathbf{p}^T = \mathbf{p}_{n*}^i$ according to (18)
12:    **for** $n = 1$ to N_{pop} **do**
13:      Calculate $\mathbf{p}_{n,new}$ acordind to (20) and $f_{n,new}$ via (23)
14:      **if** $f_{n,new} > f_n^i$ **then**
15:        set $\mathbf{p}_{n,out}^T = \mathbf{p}_{n,new}$ and $f_{n,out}^T = f_{n,new}$
16:        **if** $f_{n,out}^T > f_{best}^i$ **then**
17:          set $\mathbf{p}_{best}^i = \mathbf{p}_{n,out}^T$ and $f_{n,best}^i = f_{n,out}^T$
18:        **end if**
19:      **else**
20:        set $\mathbf{p}_{n,out}^T = \mathbf{p}_n^i$ and $f_{n,out}^T = f_n^i$
21:      **end if**
22:    **end for**
23:    $\triangleright$ Learning stage
24:    **for** $n = 1$ to N_{pop} **do**
25:      Select learner m randomly ($m \neq n$)
26:      Calculate $\triangle \mathbf{p}$ via (21)
27:      Calculate $\mathbf{p}_{n,new}$ according to (22) and $f_{n,new}$ via (23)
28:      **if** $f_{n,new} > f_{n,out}^T$ **then**
29:        $\mathbf{p}_n^{i+1} = \mathbf{p}_{n,new}$ and $f_n^{i+1} = f_{n,new}$
30:        **if** $f_n^{i+1} > f_{best}^i$ **then**
31:          $\mathbf{p}_{best}^{i+1} = \mathbf{p}_n^{i+1}$ and $f_{best}^{i+1} = f_n^{i+1}$
32:        **else**
          $\mathbf{p}_{best}^{i+1} = \mathbf{p}_{best}^i$ and $f_{best}^{i+1} = f_{best}^i$
33:        **end if**
34:      **else**
35:        $\mathbf{p}_n^{i+1} = \mathbf{p}_n^T$ and $f_n^{i+1} = f_{n,out}^T$
36:      **end if**
37:    **end for**
38:    **if** $\eta_{EE}(\mathbf{p}_{best}^{i+1}) - \eta_{EE}(\mathbf{p}_{best}^i) \leq \varepsilon$ **then**
39:      $\mathbf{p}^* = \mathbf{p}_{best}^{i+1}$ and $\eta_{EE}^* = \eta_{EE}(\mathbf{p}_{best}^{i+1})$
40:      break
41:    **end if**
42:    $i = i + 1$
43: **end while**
44: **Return** $\mathbf{p}^*$ and η_{EE}^*

where $h_0 = \dfrac{\gamma_{th}}{\max_{\mu}\left(p_{j_c,\mu} - \sum_{t=\mu+1}^{K} p_{j_c,t}\gamma_{th}\right)}$, and the cumulative

distribution function (CDF) $F_{h_k}(h)$ is given by

$$F_{h_k}(h) = 1 + \prod_{j_c=1}^{N_c}\left(\frac{a_{j_c,k}}{b_{j_c,k}}\right)^{a_{j_c,k}} \bar{H}_{N_c+1,N_c+1}^{0,N_c+1}\left[e^h \left| \begin{matrix} \frac{I}{\Xi_{N_c,k}^{(1)},(1,1,1)} \\ \frac{I}{\Xi_{N_c,k}^{(2)},(0,1,1)} \end{matrix}\right.\right]$$
(31)

where $\bar{H}$ is the Fox's function [42], and the coefficient sets $\Xi_{n,k}^{(1)}$ and $\Xi_{n,k}^{(2)}$, $n \in N$ are defined as:

$$\Xi_{n,k}^{(1)} = \overbrace{(1 - \frac{a_{j_c,k}}{\tilde{\Omega}_{1,k}}, 1, a_{j_c,k}), ..., (1 - \frac{a_{j_c,k}}{\tilde{\Omega}_{n,k}}, 1, a_{j_c,k})}^{n-bracketed\ terms} \quad (32)$$

and

$$\Xi_{n,k}^{(2)} = \overbrace{(\frac{a_{j_c,k}}{\tilde{\Omega}_{1,k}}, 1, a_{j_c,k}), ..., (-\frac{a_{j_c,k}}{\tilde{\Omega}_{n,k}}, 1, a_{j_c,k})}^{n-bracketed\ terms}. \quad (33)$$

When fading parameter takes integer values, the Fox's $\bar{H}$ function reduces to the familiar Meijer's function G [43] and (31) can be expressed as:

$$F_{h_k}(h) = \prod_{j_c=1}^{N_c}\left(\frac{a_{j_c,k}}{b_{j_c,k}}\right)^{a_{j_c,k}} \bar{G}_{\hat{N}+1,\hat{N}+1}^{\hat{N}+1,0}\left[e^{-h} \left| \begin{matrix} \Psi_{\hat{N},k}^{(1)}, 1 \\ \Psi_{\hat{N},k}^{(2)}, 0 \end{matrix}\right.\right],$$
(34)

where $\hat{N} = N_c \times a_{j_c,k}$ and the coefficient sets $\Psi_{n,k}^{(1)}$ and $\Psi_{n,k}^{(2)}$, $k \in N$ are defined as:

$$\Psi_{n,k}^{(1)} = \overbrace{(1 + \frac{a_{j_c,k}}{\tilde{\Omega}_{1,k}}), ..., (1 + \frac{a_{j_c,k}}{\tilde{\Omega}_{1,k}})}^{a_{j_c,k}-times}, \cdots$$
$$\cdots, \overbrace{(1 + \frac{a_{j_c,k}}{\tilde{\Omega}_{N_c,k}}), ..., (1 + \frac{a_{j_c,k}}{\tilde{\Omega}_{N_c,k}})}^{a_{j_c,k}-times}, \quad (35)$$

$$\Psi_{n,k}^{(2)} = \overbrace{(\frac{a_{j_c,k}}{\tilde{\Omega}_{1,k}}), ..., (\frac{a_{j_c,k}}{\tilde{\Omega}_{1,k}})}^{a_{j_c,k}-times}, \cdots, \overbrace{(\frac{a_{j_c,k}}{\tilde{\Omega}_{N_c,k}}), ..., (\frac{a_{j_c,k}}{\tilde{\Omega}_{N_c,k}})}^{a_{j_c,k}-times} \quad (36)$$

On the other hand, the improbability of the system outage will happen if all users can decode their signal, and the procedure of SIC is properly performed. Therefore, it is given by

$$P_{out}^c = \prod_{k=1}^{K} P_{suc}^k = \prod_{k=1}^{K}\left(1 - F_{h_k}(h_0)\right), \quad (37)$$

where P_{out}^c is the complement of P_{out}. Therefore, the close form of outage probability for the proposed system is obtained as:

$$P_{out} = 1 - \prod_{k=1}^{K}\left(1 - F_{h_k}(h_0)\right). \quad (38)$$

VI. NUMERICAL RESULTS AND SIMULATIONS

In this section, numerical results are provided to assess the suggested UR selection and power allocation approaches under different parameters of the system. The results for EE, SE, their trade-off, the convergence speed of the used algorithms and OP are provided. The Monte-Carlo simulation runs is 10^5. The main simulation parameters are given in Table III [33], [44] - [45].

TABLE III
SIMULATION PARAMETERS

Parameter	Value
Satellite transmission power (P_s)	80 W
UR transmission power	3 W
Number of URs (J)	10
Number of CoMP relays (N_c)	3
Number of UEs (K)	2
Noise power	-174 dBm/Hz
Path-loss component	4
Minimum SE of the weak UE	3 bit/sec/Hz
Minimum SE of the strong UE	5 bit/sec/Hz

A. Energy Efficiency Performance

Fig. 2 depicts the EE versus UAV relay height that shows the decreasing behavior of EE with increasing UR height due to the path loss. Fig. 2(a), compares the EE of the sub-optimal relay selection presented in Algorithm 1 with the optimal case. The transmission powers are obtained by the optimal method. As we can see, the sub-optimal curve has a slight difference from the optimal one, about three percent. Besides, as mentioned before, the sub-optimal relay selection decreases the complexity. Hence, it is preferred for the following simulations. In Fig. 2(b), the EE performance of the LMO, TLBO and optimal power allocation methods is investigated. As illustrated in the magnified area, there is a negligible gap among the curves of the two sub-optimal methods including LMO and TLBO compared to the optimal one. The difference is smaller in the TLBO method.

Fig. 3 shows the EE performance of the proposed TLBO algorithm in different situations, i.e., UR height, power budget per UR and the number of UR. Fig. 3(a) shows the EE per UE with variant CoMP orders in different UR heights. In general, the EE curve is decreasing with respect to the height of UR due to path loss, the amount of the drop in the non-CoMP transmission is more tangible than CoMPs. This means that, the non-CoMP transmission is more sensitive to an increase of the UR height. From (6), it is observable that an increase of CoMP order leads to growth in the circuit power of the system, p_{cir}. Hence, the non-CoMP curve placed higher than CoMP curve. Nevertheless, it will be shown in Fig. 7 that increment of the CoMP order significantly reduces the outage probability. Fig. 3(b) shows the comparison of EE performance with different heights of UR for power budgets per UR. Note that with the increase of transmitted power, the EE performance is enhanced. This enhancement is more remarkable at the lower height of the URs due to less path loss. The effect of both URs height and the number of existing URs on the EE for the 3-CoMP scenario is shown in Fig. 3(c). It can be seen that both increasing in the number of UAVs and decreasing in the UR height have a positive effect on the EE, and vice versa. As the number of URs increases, the selection of URs with better channel conditions becomes more likely.
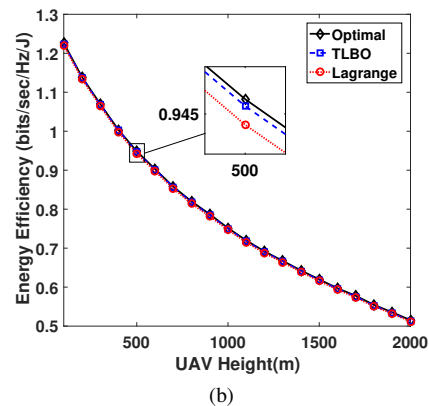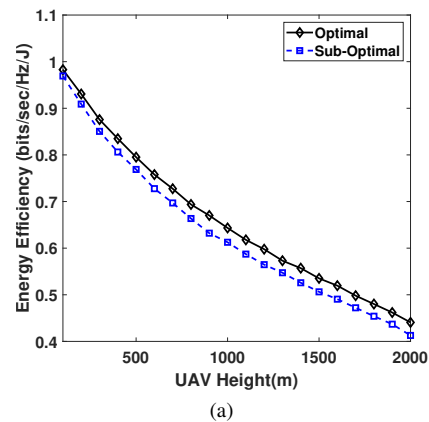

Fig. 2. Energy efficiency versus height of UAV relays: (a) Optimal and sub-optimal comparison of relay selection (b) EE of the TLBO and Lagrange methods compared to the optimal case.

B. Spectral Efficiency Performance

In Fig. 4, the SE value in different CoMP orders are compared versus UR height. Flying URs in the higher height leads to more path loss, hence, degrading SINR. Since the SE is mainly determined by UEs SINR, the SE is decreased accordingly. Furthermore, with the growth of CoMP order, the SE of UEs improves significantly, which is verified based on (2).

## C. Spectral and Energy Efficiency Trade-Off

In this part, the EE and SE trade-off for the HSURN is analyzed. From Fig. 5, we can see that the EE is equal to its optimal value until SE reaches to the threshold point, i.e., $R_{sum}(p^*_{\hat{j}_c,k})$, after that, EE begins to decline. The reason is that just for SE values below the SE threshold, the optimal EE of the system can satisfy the minimum SE requirements. For values higher than SE threshold, the system consumes more power than $p^*_{\hat{j}_c,k}$, causing the EE degradation. Comparing CoMP transmission modes in Fig. 5(a) shows that the EE drops significantly in larger SE values as the CoMP order grows, i.e., CoMP scenario can preserve EE in optimal value for a wider range of SE. In Fig. 5(b) EE for 3-CoMP transmission scenario in different UR heights is shown. As illustrated, in lower heights of UR due to the stronger link between UR and UE, the EE curve drops for greater value of SE.
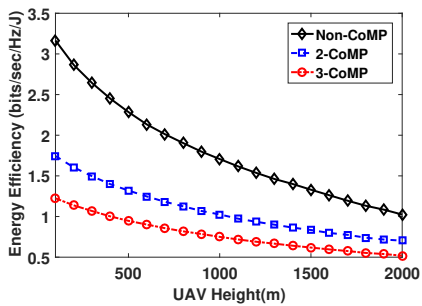
(a)
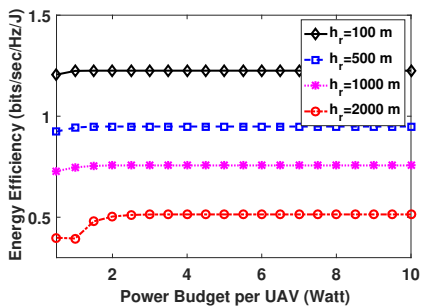
(b)
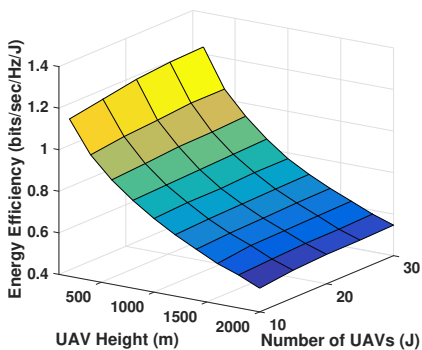
(c)

Fig. 3. EE performance for variant situations. (a) EE versus UAV height. (b) EE versus power budget per UR. (c) Comparison of the EE in UAV height and number of UAVs.
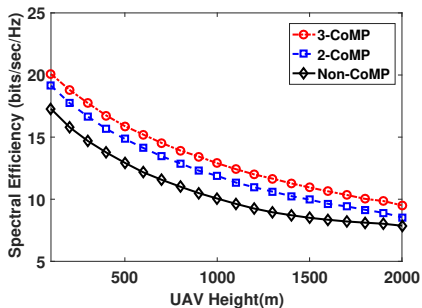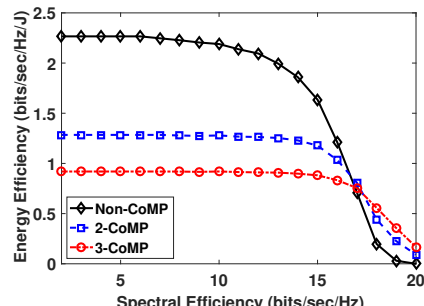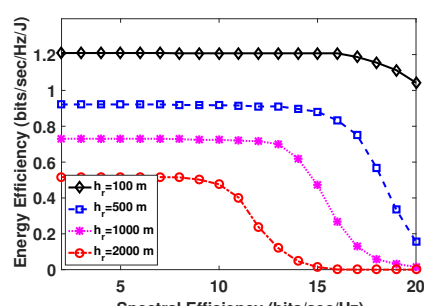

Fig. 4. The SE performance for different URs height.

D. Convergence Analysis

In Fig. 6, the convergence speed for the EE optimization problem through both TLBO and Lagrange algorithms is shown. The results for different heights of URs are averaged. Both algorithms converge after a few iterations, but the convergence speed of the TLBO algorithm is more than LMO.
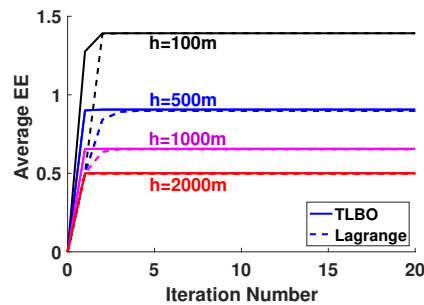

(a)

(b)

Fig. 5. Trade-off between the EE and SE of UEs. (a). In different order of CoMP. (b). In different UR height.

(a)

Fig. 6. Convergence speed of TLBO and LMO algorithms.

E. Outage Probability Performance

In Fig. 7, the effect of CoMP-NOMA transmission on outage probability is investigated. Since the CoMP transmission improves diversity gain and raises the LoS link between URs and UEs, it leads to a decrease in OP and more reliable communication. In Fig. 7(a), outage probability versus different heights of URs is shown considering the transmitted power as -3 dB. In a practical application, increasing the URs height causes to degrade the OP because of path loss. Fig. 7(b) demonstrates the decreasing of the system OP versus the increasing of the transmitted power per UR for the height of 500m in which the curves drop faster in the CoMP cases.

VII. CONCLUSION

In this paper, we considered the HSURN with JT-CoMP among selected URs to serve terrestrial NOMA users. Our goal was to maximize the EE of the suggested model via UR selection and power allocation approaches. For this end, we have proposed a sub-optimal relay selection scheme. Then,
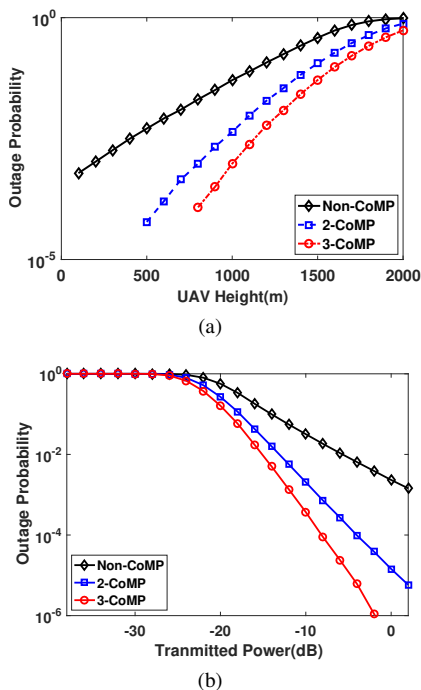
Fig. 7. Outage probability performance for variant CoMP order. (a) OP versus UR height. (b). OP versus transmitted power.

to avoid the complexity of the non-convex EE problem, we utilized the TLBO algorithm. We also derived an analytical analysis for the outage probability of the system. Numerical results verified the effectiveness of the proposed sub-optimal relay selection and utilized power allocation algorithm. The simulations also have verified that the utilized power allocation solution has performance closer to the optimal solution compared to LMO. As well as, we have shown that the CoMP scenario significantly improves the OP and SE.

APPENDIX A
CONCAVITY PROOF OF PROBLEM (12)

In the proposed approach, each UAV relay of the CoMP set optimizes its transmission power by taking into account all feasible solutions of the other CoMP-URs. Therefore, during optimization of allocated power to users by $UR_{\hat{j}_c}$, the value of $\{p_{j_c,k}\}, j_c \neq \hat{j}_c$ have not effect on the behavior of the objective function and can be ignored. According to these conditions, we focus on the concavity of the following objective function:

$$\{p^*_{\hat{j}_c,k}\} = \underset{\{p_{\hat{j}_c,k}\}}{\arg\max} \left(\sum_{k=1}^{K} (c_k \log_2(\frac{p_{\hat{j}_c,k}\tilde{h}_{\hat{j}_c,k}}{\sum_{t=k+1}^{K} p_{\hat{j}_c,t}\tilde{h}_{\hat{j}_c,k}+1}) + d_k) \right.$$
$$\left. -q(\sum_{k=1}^{K} p_{\hat{j}_c,k} + p_{cir}) \right), \quad (39)$$

As we can see, the last term $-q(\sum_{k=1}^{K} p_{\hat{j}_c,k} + p_{cir})$ is a linear function of $p_{\hat{j}_c,k}$, thus with the expanding of the rest terms,

we obtain

$$\sum_{k=1}^{K} (c_k \log_2(\frac{p_{\hat{j}_c,k}\tilde{h}_{\hat{j}_c,k}}{\sum_{t=k+1}^{K} p_{\hat{j}_c,t}\tilde{h}_{\hat{j}_c,k}+1})) + d_k$$

$$= \sum_{k=1}^{K} c_k \log_2(p_{\hat{j}_c,k}) + c_k \log_2(\tilde{h}_{\hat{j}_c,k}) + d_k$$

$$-c_k \log_2(\sum_{t=k+1}^{K} p_{\hat{j}_c,t}\tilde{h}_{\hat{j}_c,k}+1)), \quad (40)$$

It is obvious that the $c_k \log_2(p_{\hat{j}_c,k})$ is a concave function of variable $p_{\hat{j}_c,k}$ and the second term and third term are constant values, It is sufficient to show that the last sentence is concave. For concavity proving of this term, the following function is defined:

$$f(\mathbf{z}) \triangleq c_k \log_2(\sum_{t=k+1}^{K} e^{z_t}\tilde{h}_{\hat{j}_c,k}+1), \quad (41)$$

where $z = \ln(p_{\hat{j}_c,k}), \forall k$ and $\mathbf{z} = [z_1,...,z_K]^T$. Therefore, the Hessian matrix $\mathbf{H}$ with of $f(\mathbf{z})$ respect to $\mathbf{z}$ is

$$\mathbf{H} = \frac{c_k}{\psi^2 \ln 2} \begin{bmatrix} \psi\omega_1 - \omega_1^2 & -\omega_1\omega_2 & \cdots & -\omega_1\omega_K \\ -\omega_2\omega_1 & \psi\omega_2 - \omega_2^2 & \cdots & -\omega_2\omega_K \\ \vdots & \vdots & \ddots & \vdots \\ -\omega_K\omega_1 & -\omega_K\omega_2 & \cdots & \psi\omega_K - \omega_K^2 \end{bmatrix}$$

$$= \frac{c_k}{\psi^2 \ln 2}[\psi.diag(\boldsymbol{\omega}) - \boldsymbol{\omega}\boldsymbol{\omega}^T]_{K\times K}, \quad (42)$$

where $\boldsymbol{\omega} = [\omega_1,...,\omega_K]$, $\omega_t = p_{\hat{j}_c,t}\tilde{h}_{\hat{j}_c,k}$ and $\psi = \sum_{t=1}^{K} \omega_t + 1$. It is noteworthy that 1st to the (k-1)-th elements of $\boldsymbol{\omega}$ are zeros. By assuming of an $K \times 1$ arbitrary vector $\boldsymbol{\theta} = [\theta_1,...,\theta_K]^T$, we reach to:

$$\boldsymbol{\theta}^T \mathbf{H} \boldsymbol{\theta}$$
$$= \frac{c_k}{\psi^2 \ln 2} \left[\psi \sum_{t=1}^{K} \theta_t^2 \omega_t - \left(\sum_{t=1}^{K} \theta_t \omega_t \right)^2 \right]$$
$$> \frac{c_k}{\psi^2 \ln 2} \left[\left(\sum_{t=1}^{K} \omega_t \right) \left(\sum_{t=1}^{K} \theta_t^2 \omega_t \right) - \left(\sum_{t=1}^{K} \theta_t \omega_t \right)^2 \right]$$
$$= \frac{c_k}{\psi^2 \ln 2} \left[\left(\sum_{t=1}^{K} (\sqrt{\omega_t})^2 \right) \left(\sum_{t=1}^{K} (\theta_t \sqrt{\omega_t})^2 \right) - \left(\sum_{t=1}^{K} \theta_t \omega_t \right)^2 \right]$$
$$\geq 0, \quad (43)$$

where in the last inequality, an upper bound according to the Cauchy-Schwartz inequality by applying $\mathbf{a} = \sqrt{\boldsymbol{\omega}}$ and $\mathbf{b} = \boldsymbol{\theta}^T \sqrt{\boldsymbol{\omega}}$ are employed that holds $(\mathbf{a}^T\mathbf{a})(\mathbf{b}^T\mathbf{b}) \geq (\mathbf{a}^T\mathbf{b})^2$. As we can observe $\boldsymbol{\theta}^T \mathbf{H} \boldsymbol{\theta} \geq 0$ for any $\boldsymbol{\theta}$. Hence, the Hessian matrix $\mathbf{H}$ is positive semi-definite. Thus, $f(\mathbf{z})$ is a convex function of $\mathbf{z}$ and $-f(\mathbf{z})$ is concave. Therefore, the objection function in (40) is concave with respect to z. On the other hands, for specific q at each iteration, the object function and constraints in (12) are concave. So, this equation is a concave optimization problem.

REFERENCES

[1] F. Tang, L. Chen, X. Li, L. T. Yang, and L. Fu, "Intelligent spectrum assignment based on dynamical cooperation for 5g-satellite integrated networks," *IEEE Transactions on Cognitive Communications and Networking*, vol. 6, no. 2, pp. 523–533, 2020.

[2] M. Y. Arafat and S. Moh, "Routing protocols for unmanned aerial vehicle networks: A survey," *IEEE Access*, vol. 7, pp. 99 694–99 720, 2019.

[3] N. Zhao, W. Lu, M. Sheng, Y. Chen, J. Tang, F. R. Yu, and K.-K. Wong, "Uav-assisted emergency networks in disasters," *IEEE Wireless Communications*, vol. 26, no. 1, pp. 45–51, 2019.

[4] M. Liu, G. Gui, N. Zhao, J. Sun, H. Gacanin, and H. Sari, "Uav-aided air-to-ground cooperative nonorthogonal multiple access," *IEEE Internet of Things Journal*, vol. 7, no. 4, pp. 2704–2715, 2019.

[5] S. Mirbolouk, M. A. Choukali, M. Valizadeh, and M. C. Amirani, "Relay selection for comp-noma transmission in satellite and uav cooperative networks," in *2020 28th Iranian Conference on Electrical Engineering (ICEE)*. IEEE, 2020, pp. 1–5.

[6] T. Park, G. Lee, W. Saad, and M. Bennis, "Sum-rate and reliability analysis for power-domain non-orthogonal multiple access (pd-noma)," *IEEE Internet of Things Journal*, 2021.

[7] S. Bassoy, H. Farooq, M. A. Imran, and A. Imran, "Coordinated multi-point clustering schemes: A survey," *IEEE Communications Surveys & Tutorials*, vol. 19, no. 2, pp. 743–764, 2017.

[8] R. Ge, D. Bian, J. Cheng, K. An, J. Hu, and G. Li, "Joint user pairing and power allocation for noma-based geo and leo satellite network," *IEEE Access*, vol. 9, pp. 93 255–93 266, 2021.

[9] Z. Gao, A. Liu, C. Han, and X. Liang, "Sum rate maximization of massive mimo noma in leo satellite communication system," *IEEE Wireless Communications Letters*, 2021.

[10] H. Li, S. Zhao, Y. Li, and C. Peng, "Sum secrecy rate maximization in noma-based cognitive satellite-terrestrial network," *IEEE Wireless Communications Letters*, vol. 10, no. 10, pp. 2230–2234, 2021.

[11] Q. Huang, M. Lin, J.-B. Wang, T. A. Tsiftsis, and J. Wang, "Energy efficient beamforming schemes for satellite-aerial-terrestrial networks," *IEEE Transactions on Communications*, vol. 68, no. 6, pp. 3863–3875, 2020.

[12] X. Zhu, C. Jiang, L. Kuang, N. Ge, and J. Lu, "Non-orthogonal multiple access based integrated terrestrial-satellite networks," *IEEE Journal on Selected Areas in Communications*, vol. 35, no. 10, pp. 2253–2267, 2017.

[13] X. Yan, H. Xiao, K. An, G. Zheng, and W. Tao, "Hybrid satellite terrestrial relay networks with cooperative non-orthogonal multiple access," *IEEE Communications Letters*, vol. 22, no. 5, pp. 978–981, 2018.

[14] X. Zhang, B. Zhang, K. An, B. Zhao, Y. Jia, Z. Chen, and D. Guo, "On the performance of hybrid satellite-terrestrial content delivery networks with non-orthogonal multiple access," *IEEE Wireless Communications Letters*, vol. 10, no. 3, pp. 454–458, 2020.

[15] J. Zhao, X. Yue, S. Kang, and W. Tang, "Joint effects of imperfect csi and sic on noma based satellite-terrestrial systems," *IEEE Access*, vol. 9, pp. 12 545–12 554, 2021.

[16] R. Liu, K. Guo, K. An, S. Zhu, and H. Shuai, "Noma-based integrated satellite-terrestrial relay networks under spectrum sharing environment," *IEEE Wireless Communications Letters*, vol. 10, no. 6, pp. 1266–1270, 2021.

[17] H. Shuai, K. Guo, K. An, and S. Zhu, "Noma-based integrated satellite terrestrial networks with relay selection and imperfect sic," *IEEE Access*, vol. 9, pp. 111 346–111 357, 2021.

[18] F. Cui, Y. Cai, Z. Qin, M. Zhao, and G. Y. Li, "Multiple access for mobile-uav enabled networks: Joint trajectory design and resource allocation," *IEEE Transactions on Communications*, vol. 67, no. 7, pp. 4980–4994, 2019.

[19] M. Jia, Q. Gao, Q. Guo, and X. Gu, "Energy-efficiency power allocation design for uav assisted spatial noma," *IEEE Internet of Things Journal*, 2020.

[20] X. Chen, Z. Yang, N. Zhao, Y. Chen, J. Wang, Z. Ding, and F. R. Yu, "Secure transmission via power allocation in noma-uav networks with circular trajectory," *IEEE Transactions on Vehicular Technology*, vol. 69, no. 9, pp. 10 033–10 045, 2020.

[21] Q.-V. Pham, T. Huynh-The, M. Alazab, J. Zhao, and W.-J. Hwang, "Sum-rate maximization for uav-assisted visible light communications using noma: Swarm intelligence meets machine learning," *IEEE Internet of Things Journal*, vol. 7, no. 10, pp. 10 375–10 387, 2020.

[22] Z. Yang, Z. Ding, Y. Wu, and P. Fan, "Novel relay selection strategies for cooperative noma," *IEEE Transactions on Vehicular Technology*, vol. 66, no. 11, pp. 10 114–10 123, 2017.

[23] M. Yang, J. Chen, L. Yang, L. Lv, B. He, and B. Liu, "Design and performance analysis of cooperative noma with coordinated direct and relay transmission," *IEEE Access*, vol. 7, pp. 73 306–73 323, 2019.

[24] W. Wang, J. Tang, N. Zhao, X. Liu, X. Y. Zhang, Y. Chen, and Y. Qian, "Joint precoding optimization for secure swipt in uav-aided noma networks," *IEEE Transactions on Communications*, vol. 68, no. 8, pp. 5028–5040, 2020.

[25] N. Zhao, X. Pang, Z. Li, Y. Chen, F. Li, Z. Ding, and M.-S. Alouini, "Joint trajectory and precoding optimization for uav-assisted noma networks," *IEEE Transactions on Communications*, vol. 67, no. 5, pp. 3723–3735, 2019.

[26] M. S. Ali, E. Hossain, A. Al-Dweik, and D. I. Kim, "Downlink power allocation for comp-noma in multi-cell networks," *IEEE Transactions on Communications*, vol. 66, no. 9, pp. 3982–3998, 2018.

[27] M. Elhattab, M. A. Arfaoui, and C. Assi, "A joint comp c-noma for enhanced cellular system performance," *IEEE Communications Letters*, vol. 24, no. 9, pp. 1919–1923, 2020.

[28] M. Elhattab, M.-A. Arfaoui, and C. Assi, "Comp transmission in downlink noma-based heterogeneous cloud radio access networks," *IEEE Transactions on Communications*, vol. 68, no. 12, pp. 7779–7794, 2020.

[29] M. Elhattab, M. A. Arfaoui, C. Assi, and A. Ghrayeb, "Reconfigurable intelligent surface assisted coordinated multipoint in downlink noma networks," *IEEE Communications Letters*, 2020.

[30] A. Kilzi, J. Farah, C. A. Nour, and C. Douillard, "Mutual successive interference cancellation strategies in noma for enhancing the spectral efficiency of comp systems," *IEEE Transactions on Communications*, vol. 68, no. 2, pp. 1213–1226, 2019.

[31] Y. Al-Eryani, E. Hossain, and D. I. Kim, "Generalized coordinated multipoint (gcomp)-enabled noma: Outage, capacity, and power allocation," *IEEE Transactions on Communications*, vol. 67, no. 11, pp. 7923–7936, 2019.

[32] A. Abdi, W. C. Lau, M.-S. Alouini, and M. Kaveh, "A new simple model for land mobile satellite channels: First-and second-order statistics," *IEEE Transactions on Wireless Communications*, vol. 2, no. 3, pp. 519–528, 2003.

[33] T. Hou, Y. Liu, Z. Song, X. Sun, and Y. Chen, "Uav-to-everything (u2x) networks relying on noma: A stochastic geometry model," *IEEE Transactions on Vehicular Technology*, vol. 69, no. 7, pp. 7558–7568, 2020.

[34] M. F. Hanif, Z. Ding, T. Ratnarajah, and G. K. Karagiannidis, "A minorization-maximization method for optimizing sum rate in the downlink of non-orthogonal multiple access systems," *IEEE Transactions on Signal Processing*, vol. 64, no. 1, pp. 76–88, 2015.

[35] M. S. Ali, H. Tabassum, and E. Hossain, "Dynamic user clustering and power allocation for uplink and downlink non-orthogonal multiple access (noma) systems," *IEEE access*, vol. 4, pp. 6325–6343, 2016.

[36] Z. Zhou, M. Dong, K. Ota, J. Wu, and T. Sato, "Energy efficiency and spectral efficiency tradeoff in device-to-device (d2d) communications," *IEEE Wireless Communications Letters*, vol. 3, no. 5, pp. 485–488, 2014.

[37] F. Fang, J. Cheng, and Z. Ding, "Joint energy efficient subchannel and power optimization for a downlink noma heterogeneous network," *IEEE Transactions on Vehicular Technology*, vol. 68, no. 2, pp. 1351–1364, 2018.

[38] W. Dinkelbach, "On nonlinear fractional programming," *Management science*, vol. 13, no. 7, pp. 492–498, 1967.

[39] S. Boyd and L. Vandenberghe, *Convex optimization*. Cambridge, U.K.: Cambridge Univ. Press, 2004.

[40] R. Rao and V. Patel, "An elitist teaching-learning-based optimization algorithm for solving complex constrained optimization problems," *International Journal of Industrial Engineering Computations*, vol. 3, no. 4, pp. 535–560, 2012.

[41] R. Xue and Z. Wu, "A survey of application and classification on teaching-learning-based optimization algorithm," *IEEE Access*, vol. 8, pp. 1062–1079, 2019.

[42] R. Saxena, "Functional relations involving generalized h-function," *Le Matematiche*, vol. 53, no. 1, pp. 123–131, 1998.

[43] A. M. Mathai and R. K. Saxena, "The h function with applications in statistics and other disciplines," *John Wiley & Sons*, 1978.

[44] T. Hou, Y. Liu, Z. Song, X. Sun, and Y. Chen, "Exploiting noma for uav communications in large-scale cellular networks," *IEEE Transactions on Communications*, vol. 67, no. 10, pp. 6897–6911, 2019.

[45] G. Zheng, S. Chatzinotas, and B. Ottersten, "Generic optimization of linear precoding in multibeam satellite systems," *IEEE Transactions on Wireless Communications*, vol. 11, no. 6, pp. 2308–2320, 2012.